Fluid Dynamics and Co-located Conferences
June 24-27, 2013, San Diego, CA
21st AIAA Computational Fluid Dynamics Conference

A High-Order Implicit-Explicit Fluid-Structure Interaction Method for Flapping Flight

Bradley Froehle* and Per-Olof Persson†
University of California, Berkeley, Berkeley, CA 94720-3840, U.S.A.

We present a high-order accurate scheme for fluid-structure interaction (FSI) simulations of flapping flight. The compressible Navier-Stokes equations are discretized using a discontinuous Galerkin arbitrary Lagrangian-Eulerian (DG-ALE) method on an unstructured tetrahedral mesh, and a wing-like structure, represented as a neo-Hookean material, is discretized using standard continuous Galerkin tetrahedral elements. The time integration is performed using a partitioned approach based on an implicit-explicit Runge-Kutta method, with the fluid and structure equations each integrated using the implicit coefficients, and the fluid-to-structure coupling predicted using a combination of the implicit and explicit coefficients. This partitioned approach allows the reuse of existing domain specific efficient parallel solvers. We demonstrate up to fifth order accuracy in time on a non-trivial test problem, showing that subiterations are not required to achieve design accuracy. In addition we show several examples of wing-like structures in both two and three dimensions.

I. Introduction

In this paper, we present a high-order discontinuous Galerkin (DG) formulation for the Navier-Stokes equations coupled to a finite element model of a thin non-linear structure. Many approaches have been suggested for the simulation of fluid-structure interaction,[1,2,3] and a common way to treat the deformable domains is the use of Arbitrary Lagrangian Eulerian (ALE) methods.[4,5,6,7] In these efforts the discretization on the deformable domain is carried out on a deforming grid and thus the metric changes over time.

For the non-linear structure model we use a continuous Galerkin discretization, integrated in time simultaneously with the DG discretization. The forces from the fluid are applied to the structure, and the structure displacements provide the deformation of the fluid domain. We note that this monolithic treatment provides a time-accurate coupling, unlike other approaches where the fluid and the structure are integrated separately, and forces and displacements are only transferred at the end of each timestep.

In previous work,[8] we solved a similar problem using an explicit Runge-Kutta time integrator. While this approach is simple and does not require any coupling matrices, it may introduce undesirable timestep restrictions. However, a fully implicit time integrator would require forming not only the Jacobian matrices for the fluid and the structure problems, but also the couplings between them.

Here, we demonstrate how implicit-explicit Runge-Kutta methods[9] can be used to avoid solving the fully coupled system, with arbitrarily high orders of accuracy in time. We use both the explicit and the implicit coefficients of the schemes to form a stage predictor for the force from the fluid applied to the structure.[10] This decouples the two implicit problems for the fluid and the structure, respectively, which can be solved using standard implicit solvers.

We present the equations for both the fluid on the deforming domain and the non-linear structure. Next we describe a mesh deformation procedure based on radial basis functions, as well as the time integration procedure and the force predictor. We verify the high-order accuracy of the scheme using a test problem of a heaving and pitching NACA airfoil in a laminar flow, subject to a simple smooth heaving motion. Lastly we show simulations of flapping flight in both two and three dimensions.

*Ph.D. Candidate, Department of Mathematics, University of California, Berkeley, Berkeley CA 94720-3840. E-mail: bfroehle@berkeley.edu. AIAA Member.
†Assistant Professor, Department of Mathematics, University of California, Berkeley, Berkeley CA 94720-3840. E-mail: persson@berkeley.edu. AIAA Member.

II. Governing Equations & Discretization

II.A. Compressible Navier-Stokes

The compressible Navier-Stokes equations are written as:

$$\frac{\partial \rho}{\partial t} + \frac{\partial}{\partial x_i}(\rho u_i) = 0, \tag{1}$$

$$\frac{\partial}{\partial t}(\rho u_i) + \frac{\partial}{\partial x_i}(\rho u_i u_j + p) = +\frac{\partial \tau_{ij}}{\partial x_j} \quad \text{for } i = 1, 2, 3, \tag{2}$$

$$\frac{\partial}{\partial t}(\rho E) + \frac{\partial}{\partial x_i}\left(u_j(\rho E + p)\right) = -\frac{\partial q_j}{\partial x_j} + \frac{\partial}{\partial x_j}(u_j \tau_{ij}), \tag{3}$$

where ρ is the fluid density, u_1, u_2, u_3 are the velocity components, and E is the total energy. The viscous stress tensor and heat flux are given by

$$\tau_{ij} = \mu\left(\frac{\partial u_i}{\partial x_j} + \frac{\partial u_j}{\partial x_i} - \frac{2}{3}\frac{\partial u_k}{\partial x_j}\delta_{ij}\right) \qquad \text{and} \qquad q_j = -\frac{\mu}{\mathrm{Pr}}\frac{\partial}{\partial x_j}\left(E + \frac{p}{\rho} - \frac{1}{2}u_k u_k\right). \tag{4}$$

Here, μ is the viscosity coefficient and $\mathrm{Pr} = 0.72$ is the Prandtl number which we assume to be constant. For an ideal gas, the pressure p has the form

$$p = (\gamma - 1)\rho\left(E - \frac{1}{2}u_k u_k\right), \tag{5}$$

where γ is the adiabatic gas constant. We often use the entropy $s = p/\rho^\gamma$ for visualization. We impose two types of boundary conditions – free-stream at the far field, and adiabatic no-slip conditions at the boundaries of the structure.

II.B. Arbitrary Lagrangian Eulerian formulation

The deformable fluid domain is handled through an Arbitrary Lagrangian Eulerian (ALE) formulation. A point $\boldsymbol{X}$ in a fixed reference domain V is mapped to $\boldsymbol{x}(\boldsymbol{X}, t)$ in a time-varying domain $v(t)$.

The deformation gradient $\boldsymbol{G}$, mapping velocity $\boldsymbol{\nu}$, and mapping Jacobian g are defined as

$$\boldsymbol{G} = \nabla_{\boldsymbol{X}}\boldsymbol{x}, \qquad \boldsymbol{\nu} = \frac{\partial \boldsymbol{x}}{\partial t}, \qquad g = \det \boldsymbol{G} \tag{6}$$

A system of conservation laws in the physical domain $(\boldsymbol{x}, t)$

$$\frac{\partial \boldsymbol{u}}{\partial t} + \nabla \cdot \boldsymbol{f}(\boldsymbol{u}, \nabla \boldsymbol{u}) = 0 \tag{7}$$

is rewritten as a system of conservation laws in the reference domain $(\boldsymbol{X}, t)$

$$\frac{\partial \boldsymbol{U}}{\partial t} + \nabla_{\boldsymbol{X}} \cdot \boldsymbol{F}(\boldsymbol{U}, \nabla_{\boldsymbol{X}}\boldsymbol{U}) = 0 \tag{8}$$

where the conserved quantities and fluxes in reference space are

$$\boldsymbol{U} = g\boldsymbol{u}, \qquad \boldsymbol{F} = g\boldsymbol{G}^{-1}\boldsymbol{f} - \boldsymbol{u}\boldsymbol{G}^{-1}\boldsymbol{\nu} \tag{9}$$

and

$$\nabla \boldsymbol{u} = (\nabla_{\boldsymbol{X}}(g^{-1}\boldsymbol{U}))\boldsymbol{G}^{-T} = (g^{-1}\nabla_{\boldsymbol{X}}\boldsymbol{U} - \boldsymbol{U}\nabla_{\boldsymbol{X}}(g^{-1}))\boldsymbol{G}^{-T} \tag{10}$$

The equations are discretized in space using a high-order discontinuous Galerkin formulation with tetrahedral mesh elements and nodal basis functions. The inviscid fluxes are computed using Roe's method,[11] and the numerical fluxes for the viscous terms are chosen according to the compact discontinuous Galerkin (CDG) method.[12] After discretizing, we obtain the semi-discrete form of our equations:

$$\boldsymbol{M}^f \frac{d\boldsymbol{u}^f}{dt} = \boldsymbol{r}^f(\boldsymbol{u}^f; \boldsymbol{x}), \tag{11}$$

for solution vector $\boldsymbol{u}^f$, mass matrix $\boldsymbol{M}^f$, and residual function $\boldsymbol{r}^f(\boldsymbol{u}^f; \boldsymbol{x})$. Observe that we have written the residual function in such a way as to highlight the dependence on the ALE mesh motion $\boldsymbol{x}$. For more details see reference 13.

The geometric conservation law (GCL) can be enforced using a simple technique involving an auxiliary equation. However, since the experiments in reference 13 indicate that high-order approximation spaces are less sensitive to the GCL condition, we are for simplicity not enforcing it in our results here.

II.C. Neo-Hookean Elasticity Model

We use a non-linear hyperelastic neo-Hookean formulation[14] for modeling deformable structures. Here, the structure position is given by a mapping $\boldsymbol{x}(\boldsymbol{X}, t)$, which for each time t maps a point $\boldsymbol{X}$ in the unstretched reference configuration to its location $\boldsymbol{x}$ in the deformed configuration. From this we compute the mapping velocity and deformation gradient as

$$\boldsymbol{v} = \frac{\partial \boldsymbol{x}}{\partial t} \quad \text{and} \quad \boldsymbol{F} = \nabla_{\boldsymbol{X}} \boldsymbol{x}(\boldsymbol{X}, t). \tag{12}$$

We partition boundary of the structure domain into regions of Dirichlet and Neumann boundary conditions, $\partial V = \Gamma_D \cup \Gamma_N$. On the Dirichlet boundary Γ_D we prescribe the material position $\boldsymbol{x}_D$, or equivalently the material velocity $\boldsymbol{v}_D$. On the Neumann boundary Γ_N we allow for a general surface traction (i.e., force per unit surface area) which we denote $\boldsymbol{t}$.

The governing equations for the structure are then given by

$$\frac{\partial \boldsymbol{p}}{\partial t} - \nabla \cdot \boldsymbol{P}(\boldsymbol{F}) = \boldsymbol{b} \qquad \text{in } \Omega \tag{13}$$

$$\boldsymbol{P}(\boldsymbol{F}) \cdot \boldsymbol{N} = \boldsymbol{t} \qquad \text{on } \Gamma_N \tag{14}$$

$$\boldsymbol{x} = \boldsymbol{x}_D \qquad \text{on } \Gamma_D \tag{15}$$

where $\boldsymbol{p} = \rho \boldsymbol{v} = \rho\, \partial \boldsymbol{x}/\partial t$ is the momentum, $\boldsymbol{P}$ is the first Piola-Kirchhoff stress tensor, $\boldsymbol{b}$ is an external body force per unit reference volume, and $\boldsymbol{N}$ is a unit normal vector in the reference domain.

For a compressible neo-Hookean material the strain energy density is given by

$$W = \frac{\mu}{2}(\bar{I}_1 - 3) + \frac{\kappa}{2}(J-1)^2 \tag{16}$$

where $\bar{I}_1$, the first invariant of the deviatoric part of the left Cauchy-Green deformation tensor, and J, the determinant of the deformation gradient, are calculated as

$$\bar{I}_1 = J^{-2/3} I_1, \quad I_1 = \det \boldsymbol{B} = \det(\boldsymbol{F}\boldsymbol{F}^T), \quad \text{and} \quad J = \det \boldsymbol{F}. \tag{17}$$

The constants μ and κ are the shear and bulk modulus of the material.

The first Piola-Kirchhoff stress tensor is computed as

$$\boldsymbol{P}(\boldsymbol{F}) = \frac{\partial W}{\partial \boldsymbol{F}} = \mu J^{-2/3} \left(\boldsymbol{F} - \frac{1}{3} \operatorname{tr}(\boldsymbol{F}\boldsymbol{F}^T) \boldsymbol{F}^{-T} \right) + \kappa (J-1) J \boldsymbol{F}^{-T}. \tag{18}$$

For two dimensional problems modeling the cross-section of a long prismatic structure we use a plane strain formulation in which we treat the stretch in the third dimension as constant.[15] This results in similar set equations, requiring only a slight modification to the Piola-Kirchhoff stress tensor.

After writing the system in a first order formulation in the displacement $\boldsymbol{x}$ and momentum $\boldsymbol{p}$ variables, the equations are discretized in space using a standard high-order continuous Galerkin formulation with tetrahedral mesh elements and nodal basis functions. This results in a semi-discrete system:

$$\boldsymbol{M}^s \frac{d\boldsymbol{u}^s}{dt} = \boldsymbol{r}^s(\boldsymbol{u}^s; \boldsymbol{t}), \tag{19}$$

for solution vector $\boldsymbol{u}^s$ containing discretized positions and momenta, mass matrix $\boldsymbol{M}^s$, and residual function $\boldsymbol{r}^s(\boldsymbol{u}^s; \boldsymbol{t})$. Note in this form it is often more natural to impose the Dirichlet conditions in the momentum variables only, letting them be integrated into the corresponding changes in position.

II.D. Coupling / Radial Basis Functions

To simplify the coupling between the fluid and the structure, we insist on two critical requirements. First, we insist that the boundary faces of the two meshes are coincident. That is, along the fluid-structure boundary, each boundary face of the structure mesh directly matches a boundary face of the fluid mesh. Second, we require that the fluid and structure be discretized using the same polynomial order.

To compute the fluid-to-structure coupling we numerically evaluate the momentum flux through the boundary faces and provide the quantities to the structure solver as the surface traction. To ensure a highly accurate coupling this transfer is done at the Gaussian integration nodes, not the solution nodes.

The structure-to-fluid coupling is a deformation of the fluid mesh in response to a change in the structure position. We represent the deformed fluid mesh and mapping velocity on each element of the fluid mesh using polynomials of the same order as the fluid discretization. Since we insist that the fluid and structure are discretized using the same order polynomials, the deformed fluid mesh may *exactly* conform to the deformed structure by setting the positions of the boundary fluid nodes to the deformed position of the structure. Since the structure may undergo a large deformation, we use radial basis function interpolation[16,17] to deform the fluid mesh to maintain high element quality and prevent element inversion.

The radial basis function interpolant gives the deformed fluid position $\boldsymbol{x}$ as a function of the reference position $\boldsymbol{X}$ and has the form

$$\boldsymbol{x}(\boldsymbol{X}) = \sum_{j=1}^{n} \boldsymbol{\alpha}_j \phi(\|\boldsymbol{X} - \boldsymbol{X}_j\|_2) + \boldsymbol{p}(\boldsymbol{X}) \tag{20}$$

where $\{\boldsymbol{X}_j\}$ is a set of control points, ϕ a radial basis function, and $\boldsymbol{p}$ linear polynomial. Here we choose a compactly supported C^2 function

$$\phi(r) = \begin{cases} (1-r)^4(4r+1) & \text{if } 0 \le r \le 1 \\ 0 & \text{if } 1 \le r. \end{cases} \tag{21}$$

The coefficients $\boldsymbol{\alpha}_j$ and coefficients of the polynomial $\boldsymbol{p}$ are found by imposing the value of $\boldsymbol{x}$ at the control points $\boldsymbol{X_j}$, i.e.,

$$\boldsymbol{x}_j = \boldsymbol{x}(\boldsymbol{X}_j) \quad \text{for } j = 1, \ldots, N \tag{22}$$

and additionally requiring

$$\sum_{j=1}^{N} \boldsymbol{\alpha}_j \boldsymbol{q}(\boldsymbol{X}_j) = 0 \tag{23}$$

for all polynomials $\boldsymbol{q}$ of degree less than or equal to the degree of $\boldsymbol{p}$, i.e. 1.

The control points $\{\boldsymbol{X}_j\}$ are set to be all nodes on the boundary of the fluid mesh. Those nodes along the fluid-structure interface have their position $\boldsymbol{x}_j$ set from the current displacement of the structure. Nodes at the far-field boundary of the fluid are generally held at a fixed position.

II.E. Temporal Integrator

Consider for the moment our system of fluid $\boldsymbol{u}^f$ and structure $\boldsymbol{u}^s$ variables written as a coupled first order system of ordinary differential equations $\boldsymbol{M}\, d\boldsymbol{u}/dt = \boldsymbol{r}(\boldsymbol{u})$ where

$$\boldsymbol{u} = \begin{bmatrix} \boldsymbol{u}^f \\ \boldsymbol{u}^s \end{bmatrix}, \quad \boldsymbol{r} = \begin{bmatrix} \boldsymbol{r}^f(\boldsymbol{u}^f;\, \boldsymbol{x}(\boldsymbol{u}^s)) \\ \boldsymbol{r}^s(\boldsymbol{u}^s;\, \boldsymbol{t}(\boldsymbol{u}^f)) \end{bmatrix}, \quad \boldsymbol{M} = \begin{bmatrix} \boldsymbol{M}^f & \\ & \boldsymbol{M}^s \end{bmatrix}. \tag{24}$$

Note that we have highlighted the dependence of the fluid on the structure arising from the ALE mesh motion $\boldsymbol{x}$, and the structure on the fluid via the surface traction $\boldsymbol{t}$. Because the surface traction $\boldsymbol{t}$ enters the structure equation $\boldsymbol{r}^s$ linearly, we may rewrite the equation as

$$\boldsymbol{r}^s(\boldsymbol{u}^s;\, \boldsymbol{t}(\boldsymbol{u}^f)) = \boldsymbol{r}^{ss}(\boldsymbol{u}^s) + \boldsymbol{r}^{sf}(\boldsymbol{t}(\boldsymbol{u}^f)) \tag{25}$$

$$= \boldsymbol{r}^s(\boldsymbol{u}^s;\, \tilde{\boldsymbol{t}}) + \boldsymbol{r}^{sf}(\boldsymbol{t}(\boldsymbol{u}^f) - \tilde{\boldsymbol{t}}) \tag{26}$$

where $\tilde{\boldsymbol{t}}$ is a another surface traction. We generally think of $\tilde{\boldsymbol{t}}$ as a predicted value of $\boldsymbol{t}(\boldsymbol{u}^f)$ and refer to it as a predicted fluid-to-structure coupling.

Using this formulation, we may split equation 24 as

$$\boldsymbol{M}\frac{d\boldsymbol{u}}{dt} = \begin{bmatrix} \boldsymbol{r}^f(\boldsymbol{u}^f;\, \boldsymbol{x}(\boldsymbol{u}^s)) \\ \boldsymbol{r}^s(\boldsymbol{u}^s;\, \tilde{\boldsymbol{t}}) \end{bmatrix} + \begin{bmatrix} \\ \boldsymbol{r}^{sf}(\boldsymbol{t}(\boldsymbol{u}^f) - \tilde{\boldsymbol{t}}) \end{bmatrix} \tag{27}$$

where we intend to treat the first term implicitly and the second term explicitly using an implicit-explicit Runge-Kutta (IMEX) scheme. In this paper we investigate the ARK3, ARK4, and ARK5 coefficients of Kennedy and Carpenter.[9] We use the letter s to denote the number of stages, and the standard variable names a_{ij}, $\hat{a}_{ij}$, b_i, and c_i to denote the coefficients of the implicit scheme, explicit scheme, weights, and nodes respectively.

Our scheme differs slightly from the standard IMEX formulation in that we avoid evaluating the explicit terms $\boldsymbol{r}^{sf}$ but instead update the stage flux for the structure equation using the corrected value of the coupling $\boldsymbol{t}(\boldsymbol{u}^f)$. This naturally allows per stage Gauss-Seidel iterations where we treat the corrected fluid-to-structure coupling as the new predicted value and repeat the stage calculations. It has been reported that using one or more Gauss-Seidel iterations can improve the stability of the overall method,[18] but we emphasize that these iterations are generally not required to achieve the design accuracy of the method.

Here we use the predictor suggested by van Zuijlen et al,[10] namely the predicted value $\tilde{\boldsymbol{t}}$ at stage i is a linear combination of the corrected values $\boldsymbol{t}$ at previous stages and the implicit and explicit Runge-Kutta scheme coefficients:

$$\tilde{\boldsymbol{t}}_i = \sum_{j=1}^{i-1} \frac{\hat{a}_{ij} - a_{ij}}{a_{ii}} \boldsymbol{t}_j. \tag{28}$$

The time integration scheme is written out fully in algorithm 1. For more details see reference 19.

Algorithm 1 Time integration scheme for the FSI system in equation 24, using the s-stage implicit-explicit Runge-Kutta scheme $(a_{ij}, \hat{a}_{ij}, b_i, c_i)$. Given the structure $(\boldsymbol{u}^s_n)$ and fluid $(\boldsymbol{u}^f_n)$ values at time t_n, compute the values at $t_{n+1} = t_n + \Delta t$.

Set $\boldsymbol{t}_{n,1} = \boldsymbol{t}(\boldsymbol{u}^f_{n,1})$	▷ Evaluate fluid-to-structure coupling (surface traction)
Set $\boldsymbol{k}^s_{n,1} = M_s^{-1}\boldsymbol{r}^s(\boldsymbol{u}^s_{n,1}, \boldsymbol{t}_{n,1})$	▷ Evaluate structure residual
Set $\boldsymbol{k}^f_{n,1} = M_f^{-1}\boldsymbol{r}^f(\boldsymbol{u}^f_{n,1}, \boldsymbol{x}(\boldsymbol{u}^s_{n,1})$	▷ Evaluate fluid residual
for stage $i = 2, \ldots, s$ **do**	
Set $\tilde{\boldsymbol{t}}_{n,i} = \sum_{j=1}^{i-1} \frac{\hat{a}_{ij} - a_{ij}}{a_{ii}} \boldsymbol{t}_{n,j}$	▷ Predict the fluid-to-structure coupling
Solve for $\boldsymbol{k}^s_{n,i}$ in $M_s\boldsymbol{k}^s_{n,i} = \boldsymbol{r}^s(\boldsymbol{u}^s_{n,i}, \tilde{\boldsymbol{t}}_{n,i})$	▷ Implicit structure solve
where $\boldsymbol{u}^s_{n,i} = \boldsymbol{u}^s_n + \Delta t \sum_{j=1}^{i} a_{ij}\boldsymbol{k}^s_{n,j}$	
Solve for $\boldsymbol{k}^f_{n,i}$ in $M_f\boldsymbol{k}^f_{n,i} = \boldsymbol{r}^f(\boldsymbol{u}^f_{n,i}, \boldsymbol{x}(\boldsymbol{u}^s_{n,i}))$	▷ Implicit fluid solve
where $\boldsymbol{u}^f_{n,i} = \boldsymbol{u}^f_n + \Delta t \sum_{j=1}^{i} a_{ij}\boldsymbol{k}^f_{n,j}$	
Set $\boldsymbol{t}_{n,i} = \boldsymbol{t}(\boldsymbol{u}^f_{n,i})$	▷ Correct the fluid-to-structure coupling
Set $\boldsymbol{k}^s_{n,i} = M_s^{-1}\boldsymbol{r}^s(\boldsymbol{u}^s_{n,i}, \boldsymbol{t}_{n,i})$	▷ Re-evaluate structure residual
end for	
Set $\boldsymbol{u}^s_{n+1} = \boldsymbol{u}^s_n + \Delta t \sum_{i=1}^{s} b_i\boldsymbol{k}^s_{n,i}$	▷ Advance structure
Set $\boldsymbol{u}^f_{n+1} = \boldsymbol{u}^f_n + \Delta t \sum_{i=1}^{s} b_i\boldsymbol{k}^f_{n,i}$	▷ Advance fluid

III. Results

III.A. Pitching and Heaving Airfoil

To validate the high-order convergence in time, we consider a simple test problem consisting of a pitching and heaving NACA 0012 airfoil. The airfoil of chord length 1 is allowed rotate around a fixed pivot in the interior of the airfoil, as shown in figure 1. Since the airfoil is treated as a rigid body, the structure variables

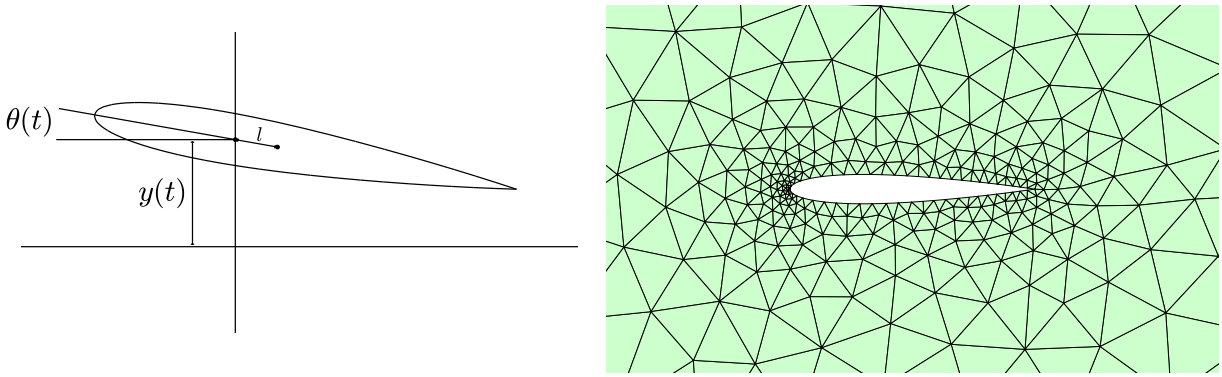

Figure 1. At left, the schematic for the pitching and heaving NACA0012 airfoil. At right, the computational reference mesh used for the fluid.

consist only of the pitching angle θ and the angular velocity ω. The fluid is assigned no-slip boundary conditions on the interface with the airfoil, which contributes a torque τ about the pivot of the airfoil.

The vertical position of the pivot follows a prescribed C^3 blending motion

$$y(t) = \begin{cases} 0 & \text{if } t \leq 0 \\ A(-20t^7 + 70t^6 - 84x^5 + 35t^4) & \text{if } 0 \leq t \leq 1 \\ A & \text{if } 1 \leq t \end{cases} \tag{29}$$

where A is the heaving amplitude. In addition the airfoil is subject to a torsional restoring force with spring constant k. The equations of motion of the structure, written as a first order system, are

$$\frac{\partial \theta}{\partial t} = \omega \tag{30}$$

$$I\frac{\partial \omega}{\partial t} = -k\theta - \tau - lm\cos(\theta)y''(t) \tag{31}$$

where I is the moment of inertia (around the pivot), l is the distance from the pivot to the center of mass, and m is the total mass of the airfoil.

The non-dimensionalized constants chosen for this problem are $I = 1$, $k = 0.1$, $l = 0.2$, $M = 1$, and $A = 1$. The airfoil has chord length 1, and the pivot located along the chord a distance $1/3$ from the leading edge. The far field fluid has non-dimensionalized velocity $\boldsymbol{u} = [1, 0]^T$, density 1, Mach 0.2, and Reynolds number 1000. The initial conditions of the airfoil are no pitching and no angular velocity, i.e, $\theta(0) = 0$ and $\omega(0) = 0$. To initialize the fluid at time $t = 0$ we freeze the structure and solve for the steady state fluid solution. The evolution of the system is shown in figure 2.

The temporal convergence of the angle of attack $\theta(t)$ was measured by comparing the solution to the results using an explicit fourth order Runge-Kutta method (RK4) with a suitably small timestep. In general we observe that we can achieve third, fourth, and fifth order accuracy using the additive Runge-Kutta methods of the same order, as can be seen in figure 3. In each case we also solved the fully-coupled (monolithic) fluid-structure system using the implicit coefficients of the scheme, by performing Gauss-Seidel subiterations until achieving numerical convergence. This resulted in a negligible increase in accuracy despite a tremendous increase in computational cost.

We emphasize that a naïve staggered method would generally achieve first, or at most second, order accuracy in time. Here, we are able to achieve up to 5th order accuracy in time while reusing the same fluid and and structure solvers that would be used in a staggered scheme.

III.B. Flapping Wing, 2D

We model a two dimensional flapping wing as a thin rectangular structure of chord length 1 and height 0.06 whose endpoints are heaved according to a prescribed vertical motion. The leading ("left") and trailing

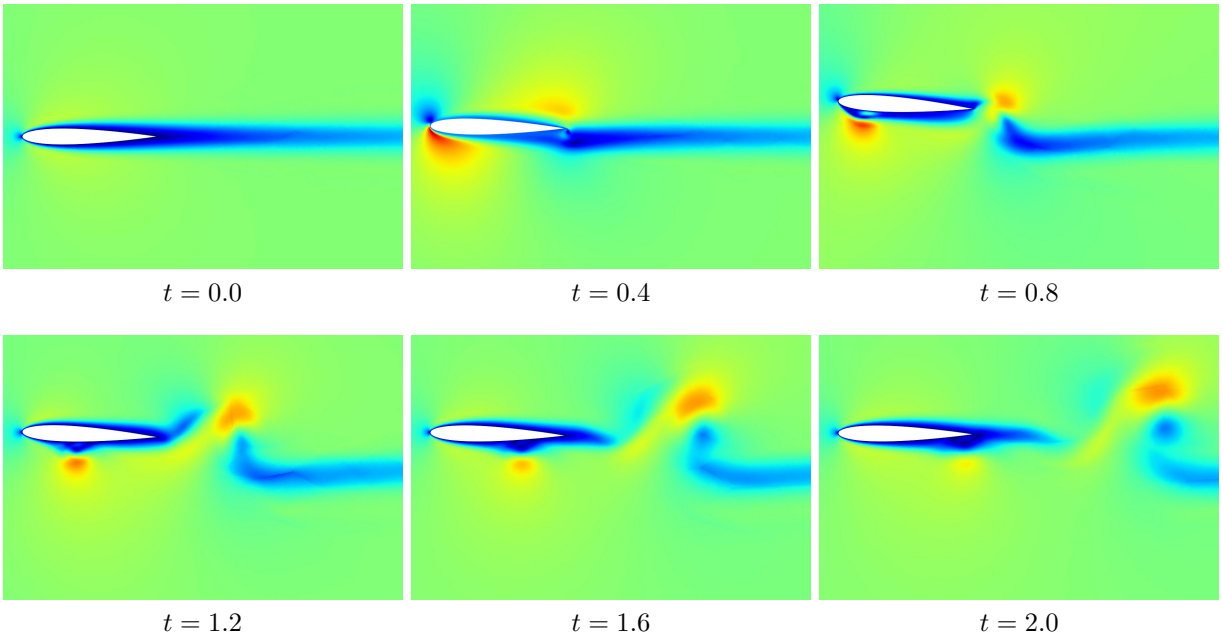

Figure 2. The airfoil at various times (Mach number). The airfoil is heaved upwards between time $t = 0$ and $t = 1$.

("right") edges follow a sinusoidal motion with a phase lag of 60°. Specifically,

$$y_l(t) = A\sin(2\pi f t) \tag{32}$$
$$y_r(t) = A\sin(2\pi f t - \phi) \tag{33}$$

where $A = 0.5$, $f = 0.2$, and $\phi = \pi/3$. A schematic of the model along with the material parameters is shown in figure 4.

For consistency in the initialization of the fluid, the structure was forced into a 0° angle of attack at time $t = 0$ by multiplying the y_l- and y_r-coordinates by a smooth C^3 blending function which was 0 at $t = 0$ and 1 at $t = 1/(4f)$. This creates a somewhat violent initial motion and in some cases introduces transient modes in the structure which decay after a few periods of heaving.

The structure was always started with no velocity and in a rectangular configuration with height $h = 0.06$ and length $l = 1$. In some cases the structure was prestretched by an amount Δ by changing the reference dimensions of the structure to $l_{ref} = l/\Delta$ and $h_{ref} = h\Delta^{2\nu}$, where ν is Poisson's ratio. This is not a stationary configuration for the structure, but the initial transients decay quickly and do not cause any difficulties in the simulation.

The structure was discretized using 44 degree 3 polynomial elements for a total of 268 nodes or 1072 degrees of freedom. The fluid was discretized using 2575 degree 3 polynomial elements for a total of 25,750 nodes or 103,000 degrees of freedom. A timestep of $\Delta t = 5 \times 10^{-3}$ was used to integrate the system until time $T = 20.0$.

We investigated several different material parameters and prestretching factors, and show the results of the simulations at several times in figure 5. Note that the varying parameters greatly impact the ability of the structure to align with the incident flow. Each simulation took approximately 3 hours on 48 CPU cores.

III.C. Flapping Wing, 3D

In three dimensions we consider a thin prismatic triangular structure of root chord length 1, tip-to-tip span length 3, thickness 0.01, and 0° sweep, as shown in figure 6. The leading edge of the wing is driven in a

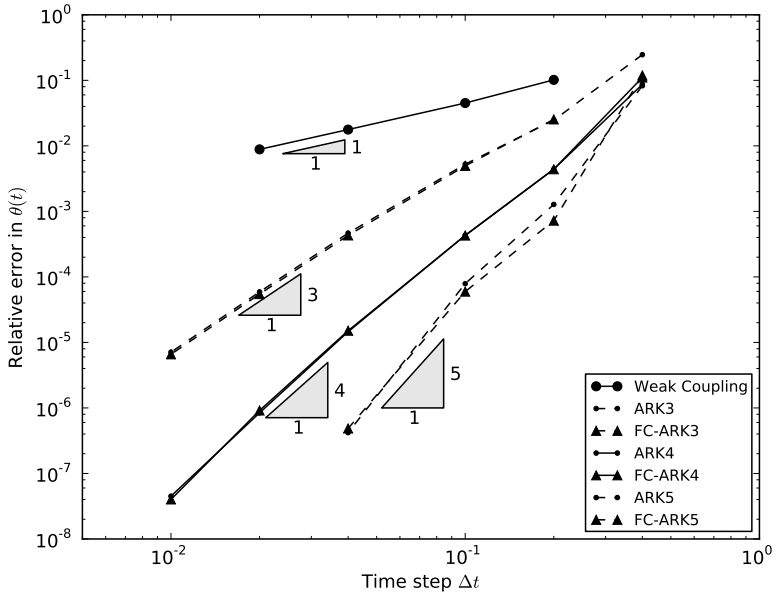

Figure 3. The relative error in angle of attack, $\|\theta(t) - \theta_{exact}(t)\|_\infty / \|\theta_{exact}(t)\|_\infty$, as a function of timestep. The ARK3, ARK4, and ARK5 schemes achieve the expected order of accuracy. Solving the fully-coupled ("FC-") system using the implicit method from the IMEX scheme shows a negligible increase in accuracy despite a large increase in computational cost. A basic staggered weak coupling scheme is shown for comparison.

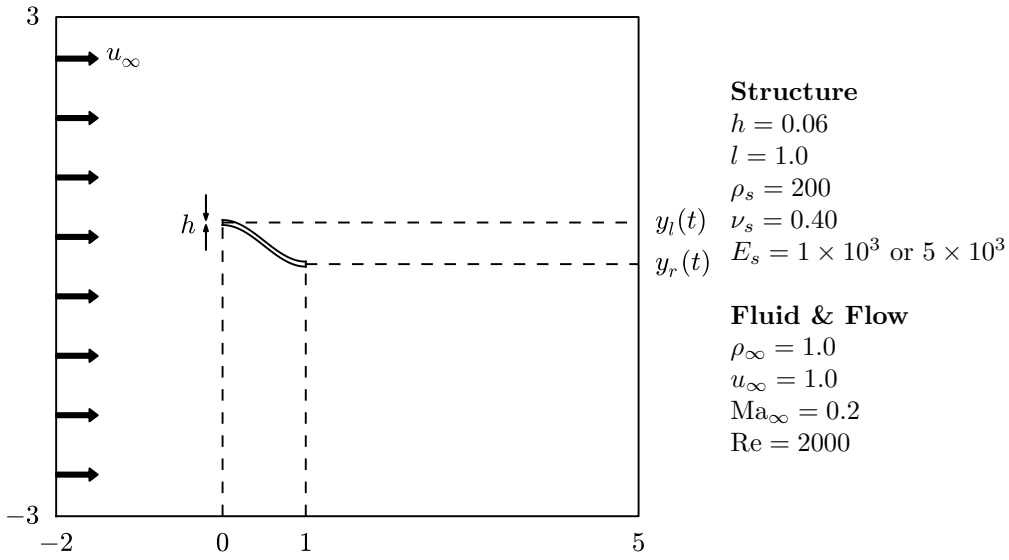

Figure 4. The two dimensional wing model in non-dimensionalized coordinates. The left and right endpoints of the structure follow a prescribed motion.

$E = 5 \times 10^3$
$\Delta = 1.5$

$E = 1 \times 10^3$
$\Delta = 1.2$

$E = 1 \times 10^3$
$\Delta = 1.1$

Figure 5. The two dimensional wing (black) at time $T = 17.0$ (top), 18.0, 19.0, and 20.0 (bottom). The structures have varying Young's modulus E and prestretching factor Δ, and range from nearly rigid (left) to quite flexible (right). (Entropy).

sinusoidal skewing motion in the y-z plane, namely

$$x(t, X, Y, Z) = X \tag{34}$$
$$y(t, X, Y, Z) = \cos(\theta(t))Y \tag{35}$$
$$z(t, X, Y, Z) = \sin(\theta(t))|Y| + Z \tag{36}$$

where the dihedral angle $\theta(t)$ follows a sinusoidal pattern

$$\theta(t) = \theta_0 \cos(2\pi f t), \tag{37}$$

with amplitude $\theta_0 = \pi/12$ and frequency $f = 0.2$.

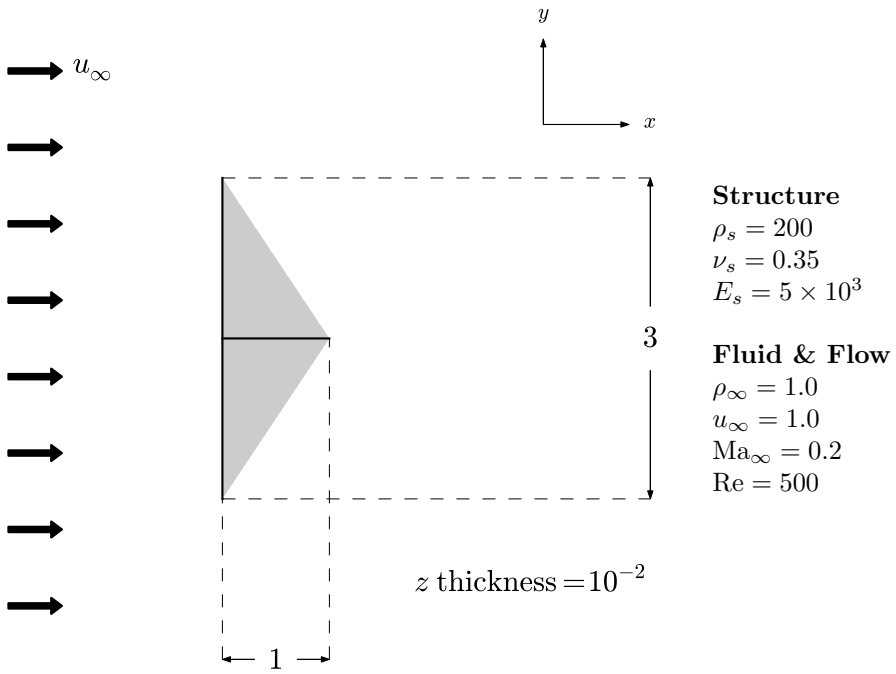

Figure 6. The overhead view of the three dimensional wing which is uniformly extruded in the z direction. Dirichlet conditions are imposed along the planes given by the solid lines. The leading edge is driven with a sinusoidal flapping motion in the y-z plane, and the root chord is held fixed.

To introduce some additional rigidity into the structure, it was prestretched by a factor Δ by changing the dimensions of the reference structure to

$$\mathrm{span}_{ref} = \mathrm{span}/\Delta \tag{38}$$
$$\mathrm{chord}_{ref} = \mathrm{chord}/\Delta \tag{39}$$
$$\mathrm{thickness}_{ref} = \mathrm{thickness}/\Delta^{-\nu}. \tag{40}$$

We used a prestretching factor $\Delta = 1.05$. To avoid strong initial transients in the structure we began the simulation by first allowing the structure to relax into a steady state configuration at the top of the flapping stroke and in the absence of the fluid.

The structure was discretized using 498 degree 2 tetrahedral elements for a total of 1197 nodes and 7182 degrees of freedom. The fluid was discretized using 22,683 degree 2 tetrahedral elements for a total of 226,830 nodes or 1,134,150 degrees of freedom. A timestep of $\Delta t = 5 \times 10^{-3}$ was used to integrate until the time $T = 5.5$ which corresponds to a little more than one complete stroke.

The simulation was run on 192 CPU cores and took approximately two hours to complete. See figure 7.

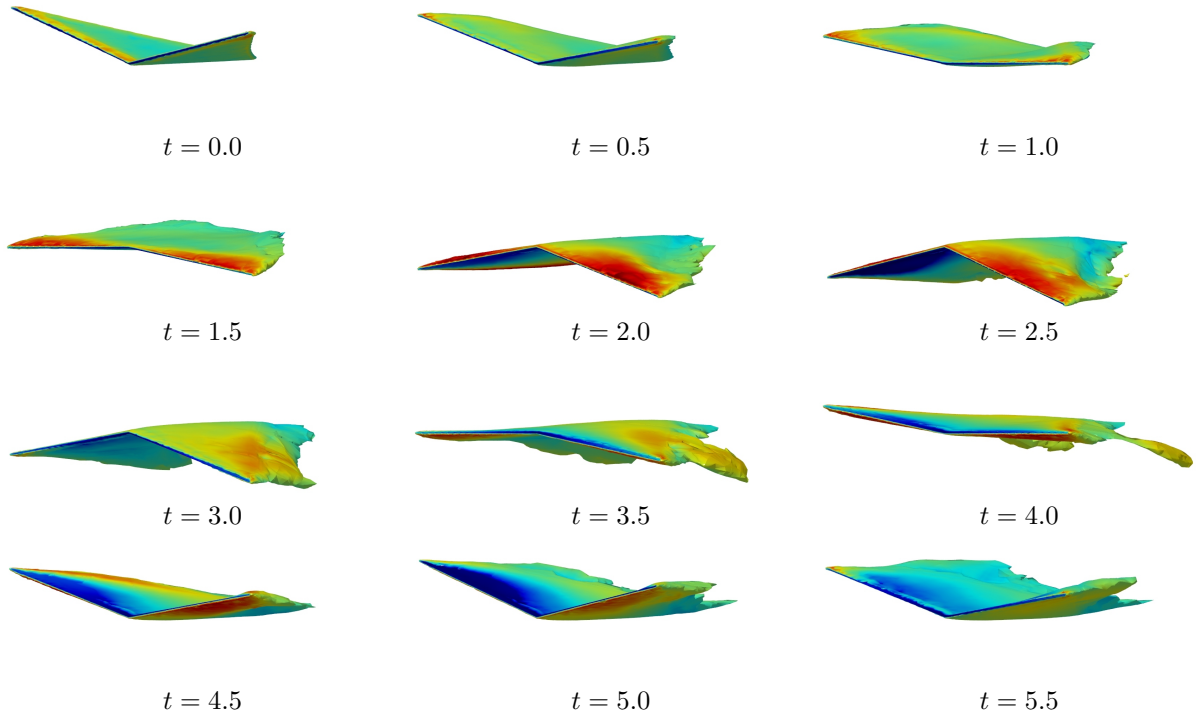

Figure 7. A three dimensional wing at various times (Mach number on iso-entropy surfaces).

Acknowledgments

We would like to acknowledge the generous support from the AFOSR Computational Mathematics program under grant FA9550-10-1-0229, the Alfred P. Sloan foundation, and the Director, Office of Science, Computational and Technology Research, U.S. Department of Energy under Contract No. DE-AC02-05CH11231.

References

[1]Yosibash, Z., Kirby, R. M., Myers, K., Szabó, B., and Karniadakis, G., "High-Order Finite Elements for Fluid-Structure Interaction Problems," *44th AIAA/ASME/ASCE/AHS Structures, Structural Dynamics, and Materials Conference, Norfolk, Virginia*, April 2003, AIAA-2003-1729.

[2]Reuther, J. J., Alonso, J. J., Martins, J. R. R. A., and Smith, S. C., "A Coupled Aero-Structural Optimization Method For Complete Aircraft Configurations," *37th AIAA Aerospace Sciences Meeting and Exhibit, Reno, Nevada*, January 1999, AIAA-99-0187.

[3]Geuzaine, P., Grandmont, C., and Farhat, C., "Design and analysis of ALE schemes with provable second-order time-accuracy for inviscid and viscous flow simulations," *J. Comput. Phys.*, Vol. 191, No. 1, 2003, pp. 206–227.

[4]Farhat, C. and Geuzaine, P., "Design and analysis of robust ALE time-integrators for the solution of unsteady flow problems on moving grids," *Comput. Methods Appl. Mech. Engrg.*, Vol. 193, No. 39-41, 2004, pp. 4073–4095.

[5]Venkatasubban, C. S., "A new finite element formulation for ALE (arbitrary Lagrangian Eulerian) compressible fluid mechanics," *Internat. J. Engrg. Sci.*, Vol. 33, No. 12, 1995, pp. 1743–1762.

[6]Lomtev, I., Kirby, R. M., and Karniadakis, G. E., "A discontinuous Galerkin ALE method for compressible viscous flows in moving domains," *J. Comput. Phys.*, Vol. 155, No. 1, 1999, pp. 128–159.

[7]Ahn, H. T. and Kallinderis, Y., "Strongly coupled flow/structure interactions with a geometrically conservative ALE scheme on general hybrid meshes," *J. Comput. Phys.*, Vol. 219, No. 2, 2006, pp. 671–696.

[8]Persson, P.-O., Peraire, J., and Bonet, J., "A High Order Discontinuous Galerkin Method for Fluid-Structure Interaction," *18th AIAA Computational Fluid Dynamics Conference, Miami, Florida*, 2007, AIAA-2007-4327.

[9]Kennedy, C. A. and Carpenter, M. H., "Additive Runge-Kutta schemes for convection-diffusion-reaction equations," *Appl. Numer. Math.*, Vol. 44, No. 1-2, 2003, pp. 139–181.

[10]van Zuijlen, A., de Boer, A., and Bijl, H., "Higher-order time integration through smooth mesh deformation for 3D fluid-structure interaction simulations," *J. Comput. Phys.*, Vol. 224, 2007, pp. 414–430.

[11]Roe, P. L., "Approximate Riemann solvers, parameter vectors, and difference schemes," *J. Comput. Phys.*, Vol. 43, No. 2, 1981, pp. 357–372.

[12]Peraire, J. and Persson, P.-O., "The compact discontinuous Galerkin (CDG) method for elliptic problems," *SIAM J. Sci. Comput.*, Vol. 30, No. 4, 2008, pp. 1806–1824.

[13]Persson, P.-O., Bonet, J., and Peraire, J., "Discontinuous Galerkin solution of the Navier-Stokes equations on deformable domains," *Comput. Methods Appl. Mech. Engrg.*, Vol. 198, 2009, pp. 1585–1595.

[14]Holzapfel, G. A., *Nonlinear solid mechanics*, John Wiley & Sons Ltd., Chichester, 2000, A continuum approach for engineering.

[15]Bonet, J. and Wood, R. D., *Nonlinear continuum mechanics for finite element analysis*, Cambridge University Press, Cambridge, 1997.

[16]Beckert, A. and Wendland, H., "Multivariate interpolation for fluid-structure-interaction problems using radial basis functions," *Aerosp. Sci. Technol.*, Vol. 5, 2001, pp. 125–134.

[17]de Boer, A., van der Schoot, M., and Bijl, H., "Mesh deformation based on radial basis function interpolation," *Comput. Struct.*, Vol. 85, 2007, pp. 784–795.

[18]van Zuijlen, A., *Fluid-Structure Interaction Simulations: Efficient Higher Order Time Integration of Partitioned Systems*, Ph.D. thesis, TU Delft, November 2006.

[19]Froehle, B. and Persson, P.-O., "A High-Order Discontinuous Galerkin Method for Fluid-Structure Interaction with Efficient Implicit-Explicit Time Stepping," Submitted for publication.